[Article] www.whxb.pku.edu.cn

铬酸及硝酸混合液处理以增强碳纳米管场发射

李世鸿 张永平* 李丽英
(大叶大学电机工程学系, 台湾 彰化 500)

摘要: 为了修饰碳纳米管(CNTs)的表面型态及改变碳纳米管的表面结构, 进一步增强碳纳米管的场发射特性, 使用铬酸及硝酸的混合溶液对碳纳米管进行后处理. 采用 SEM、TEM、Raman 和 EDS 测试手段对样品的形貌、表面成份组成和微观结构特征进行了表征. 场发射(FE)的数据显示, 经过铬酸及硝酸的混合溶液处理 20 min 的碳纳米管场发射电流比未经任何处理的碳纳米管场发射电流明显增加一个数量级以上, 场发射电流增强的主要原因为样品上的碳纳米管的表面型态的改变, 造成碳纳米管场发射增强因子 β 的增大. 与单独使用硝酸溶液后处理比较, 使用铬酸及硝酸的混合溶液对碳纳米管进行后处理可以得到较高的场发射电流及较低的起始电场. 铬酸及硝酸的混合溶液处理方法能经济且有效增强碳纳米管的场发射特性.

关键词: 铬酸; 硝酸; 碳纳米管; 场发射
中图分类号: O644

Enhancement of Field Emission Characteristics for Multi-Walled Carbon Nanotubes Treated with a Mixed Solution of Chromic Trioxide and Nitric Acid

LEE Shih-Fong CHANG Yung-Ping* LEE Li-Ying
(*Department of Electrical Engineering, Dayeh University, Changhua 500, Taiwan Province, P. R. China*)

Abstract: A simple acid treatment method was applied to functionalize the surface and to modify the structures of multi-walled carbon nanotubes (CNTs) grown on silicon substrates using a mixed solution of chromic trioxide (CrO_3) and nitric acid (HNO_3). Scanning electron microscopy (SEM), transmission electron microscopy (TEM), Raman spectroscopy, and energy dispersive spectrometer (EDS) were employed to investigate the mechanism causing the modified field emission (FE) properties of the CNT films. After 20 min of CrO_3+HNO_3 treatment, the emitted currents were enhanced by more than one order of magnitude compared with those of the untreated CNTs. This large increases in emitted current can be attributed to the favorable surface morphologies, open-ended structures, and highly curved CNT surfaces in the CNT films. These factors altogether caused an increase in the field enhancement factors of CNTs. We also demonstrated that using a mixed solution of CrO_3+HNO_3 post-treatment exhibited a higher emission current and a lower turn-on electric field than in the CNTs treated with HNO_3. The method provides a simple, economical, and effective way to enhance the CNT field emission properties.

Key Words: Chromic trioxide; Nitric acid; Carbon nanotubes; Field emission

Since carbon nanotubes (CNTs) were firstly discovered by Iijima in 1991[1], several researchers have succeeded in synthesizing multi-walled and single-walled CNTs by various chemical vapor deposition (CVD) methods. In recent years, CNTs have been of great interest to researchers owing to their remarkable structural, electronic, and mechanical properties[2]. They have also been identified as potentially useful materials for a broad range of useful devices, especially in the area of cold-cathode emission for

Received: March 25, 2008; Revised: April 29, 2008; Published on Web: June 26, 2008.
English edition available online at www.sciencedirect.com
*Corresponding author. Email: ypc@cht.com.tw; Tel: +8864-8511888 ext 2166.
大叶大学研发处研究计划资助

flat panel displays[3]. Their excellent electron emission properties can be attributed to their high aspect ratios and high chemi cal stabilities[4]. Furthermore, the electron emission properties of carbon-based materials can be altered with chemical function alization[5]. On the other hand, different kinds of chemical reactions can modify nanotube properties by effects such as charge transfer, enhanced disorder, or symmetry modification. The exposure of nanotubes to chemical molecules with reducing or oxidizing properties can modify the occupation of the electronic states of the nanotubes[6–8].

It has also been reported that CNTs can be successfully filled with chromium oxide at room temperature in open air[9,10]. The interest in this kind of study is justified by the potential applications of these nano products in batteries or in the oxidation of primary alcohols, as suggested by studies done with the analogous graphite intercalation compounds (graphite intercalated with CrO_3)[11]. However, there is no systematic study on the correlation between the surface morphology and field emission characteristics of CNTs and how they can be affected by CrO_3 solution post-treatment. In this study, we present a simple and novel procedure to modify the surface of CNTs to provide an effective method to enhance their field emission.

1 Experimental

The growth of CNTs was achieved using a thermal chemical vapor deposition (CVD) system already described by Lee *et al.*[12]. Silicon substrates (*p*-type(111), resistivity 10−25 Ω·cm, Wafer Works Corp.) were cleaned with standard Radio Corporation of America (RCA) procedure. Ni film was subsequently evaporated onto the silicon substrate as the catalyst metal. The thickness of Ni was 10 nm, which was precisely controlled with a thickness monitor. The purpose of using catalyst metal in the synthesis of CNTs has been discussed elsewhere[13]. Substrates with Ni were mounted on a ceramic holder. The specimen was placed into the quartz reactor and the chamber was pumped down to less than 0.133 Pa using a mechanical pump. Before reaching the growth temperature at 900 ℃, argon (Ar, 99.99%, San Fu Chemical Co., Ltd., Taiwan) was fed into the reactor and the temperature was gradually increased until it reached the target temperature (900 ℃) and was maintained at this temperature for 10 min for stabilization. The flow rate of argon was maintained at 1800 $cm^3 \cdot min^{-1}$. The synthesis temperature and pressure were about 900 ℃ and 1.01×10^5 Pa, respectively. After the temperature and pressure were stabilized, methane (CH_4, 99.999%, San Fu Chemical Co., Ltd., Taiwan) was introduced at a flow rate of 100 $cm^3 \cdot min^{-1}$. The growth time was 15 min. The samples were then cooled in an Ar flow ambient.

Finally, the synthesized CNTs were subsequently treated for modification at room temperature in two different solutions: CrO_3 (99.99%, Hatashi Pure Chemical Ind., Ltd.) solution (0.4 $mol \cdot L^{-1}$) and CrO_3 (0.4 $mol \cdot L^{-1}$)+HNO_3(61%, Katayama Chemical Ind., Ltd.) (15.2 $mol \cdot L^{-1}$) solution separately. The process was carried out in open air at room temperature under natural light for different times ranging from 10 to 40 min. Once the treatment time was complete, the reaction products were put in deionized water and dried in a baking box.

In this study, scanning electron microscopy (SEM) was used to analyze the microstructures in plain view. A Hitachi S-3000N was used to obtain SEM images. The specimens for transmission electron microscopy (TEM) were prepared by dispersing carbon nanotubes in acetone using an ultrasonic bath. A drop of suspension was put on a lacy carbon film supported by a copper grid. These specimens were investigated in a Philips EM-430ST electron microscope operated at 200 kV. Raman spectroscopy was employed to investigate the structural changes caused by CrO_3+HNO_3 solution treatments. Raman spectra were recorded in a 3-D nanometer scale Raman PL microspectrometer (Tokyo Instruments, INC. Nanofinder 30), whose excitation source was a 632.8 nm He-Ne laser. Electron dispersive spectrometer (EDS) (Hitachi S-3000N) was used for the identification and analysis of the chemical composition of the surface of CNTs.

The samples under test were used as the cathode in the field emission measurements. Synthesized CNTs were pasted with silver paste or carbon paste onto a glass substrate coated with conducting indium tin oxide (ITO) (Corning 1737, Corning, INC.) and dried in an oven. The glass substrate together with CNTs was mounted on a test fixture as the cathode, while an ITO glass substrate was used as the anode with an emission area of ca 0.007 cm^2. The spacing between the two electrodes was adjusted to 110 μm. To ensure accurate measurement on the emitted currents of CNTs, the measurement was carried out in high vacuum. Our previous measurement results[14] had revealed that pressure had very little effect on the measured emitted current if the measurements were carried out at a pressure of less than 0.133 Pa. In this study, the vacuum chamber was pumped down to 0.133 Pa with a mechanical pump, and subsequently pumped down to 0.133 Pa with a turbomolecular pump. A Keithley 237 source-measure unit was used to apply voltage (up to 1000 V) and to measure the emitted current with pA sensitivity, allowing for the accurate characterization of current−voltage (I−V) behavior. The Keithley 237 high-voltage source-measure unit was fully automated with a computer.

2 Results and discussion

The etching of CNTs with CrO_3 is facilitated through the following reactions. CrO_3 is water soluble in reactions (1) and (2). The formation of dichromic acid ($H_2Cr_2O_7$) and chromic acid (H_2CrO_4) during the reaction of H_2O with CrO_3 has been reported earlier[15].

$$2CrO_3+H_2O \leftrightarrow H_2Cr_2O_7 \quad (1)$$

$$CrO_3+H_2O \leftrightarrow H_2CrO_4 \quad (2)$$

Both $H_2Cr_2O_7$ and H_2CrO_4 are in dynamic equilibrium:

$$2H_2CrO_4 \leftrightarrow H_2Cr_2O_7+H_2O \quad (3)$$

When the CrO_3 concentration potential of hydrogen (PH) value is reduced, the chemical reaction tends to proceed in the forward direction to $H_2Cr_2O_7$, and vice versa. According to the ear-

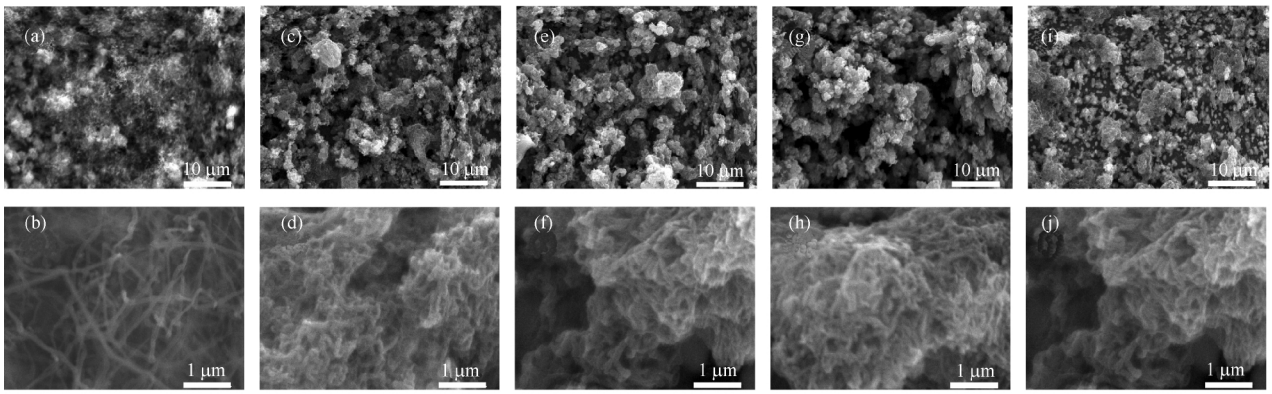

Fig.1 Typical SEM images of CNTs with different CrO_3+HNO_3 solution treatment times

(a, b) untreated; (c, d) 10 min; (e, f) 20 min; (g, h) 30 min; (i, j) 40 min

lier literature report[16], it was suggested that the reaction possibly occurred in the surface modification process as follows:

$$3C+16H^{+}+2Cr_2O_7^{2-}\leftrightarrow 4Cr^{3+}+3CO_2+8H_2O \quad (4)$$

In this reaction, Cr^{6+} was transformed into Cr^{3+} and C was transformed into CO_2. The chemical reaction of CrO_3 and CNTs involves more than one step. Slow oxidation of carbon, which is a reversible reaction, takes place first, producing several organic functional groups, such as carboxyl, phenol hydroxyl, and carbonyl, on the surfaces of CNTs. Subsequently, these organic functional groups are further oxidized and are turned into formic acid. Finally, CO_2 and water were produced through the oxygenolysis of formic acid. The reaction (4) can be verified from the observation that the CrO_3 solution, which is orange in color originally, turns into jasper after the processing, and the gas generated from the reaction can change the clear limewater into muddy water.

Firstly, changes in the surface morphologies of CNTs have been carefully examined by SEM. Fig.1 shows the top view SEM images of CNT films before and after CrO_3+HNO_3 treatment. As seen in Fig1, the configuration of nanotubes in the top layer of the film is drastically changed after CrO_3+HNO_3 solution treatment. From low resolution SEM images of Fig.1(a, c, e, g, i), it is found that CNTs modified with CrO_3+HNO_3 treatment time of 10 and 20 min have a higher surface density than that of untreated CNTs. However, for CrO_3+HNO_3 treatment time of 30 and 40 min, the surface density of CNTs and the film thickness are reduced with the increase of CrO_3+HNO_3 treatment time. The high resolution images of Fig.1 (b, d, f, h, j) show that after CrO_3+ HNO_3 treatment, the originally random CNTs on the surface become rough, blur, and tend to cluster together, which become larger, with increasing CrO_3+HNO_3 treatment time. Furthermore, it was surprisingly found that several nano-scale particles appeared along the tubes after CrO_3+HNO_3 treatment. These nano-scale particles are potential emission sites in principle.

Fig.2 depicts the TEM images showing the tip of typical multi-walled carbon nanotubes before and after 20 min of CrO_3+ HNO_3 treatment. From Fig.2(a), we can see that the Ni particle is enclosed by the graphite layers. After 20 min of CrO_3+HNO_3 treatment, the structure of CNTs changes drastically as shown in Fig.2(b). In Fig.2(b), the end of CNTs is opened by CrO_3+HNO_3 treatment and the Ni particle is diminished. Furthermore, the surfaces of CNTs become highly curved and have a high density of structure defects. This is very similar to that observed in CNTs treated by oxidization processes[17]. The open-ended structure is regarded as one of the possible factors for the observed enhancement in the FE of CNTs[18–20].

The phase composition of the CNT films, which was determined by Raman spectra, was found to be also dependent on the duration of CrO_3+HNO_3 treatment. Fig.3 shows the Raman spectra of the samples treated for different times. All spectra are dominated by two intensity peaks located at 1328 and 1580 cm^{-1}, which are referred to as the D line and G line, respectively[21]. The ratio of the intensities of D peak and G peak is an indication

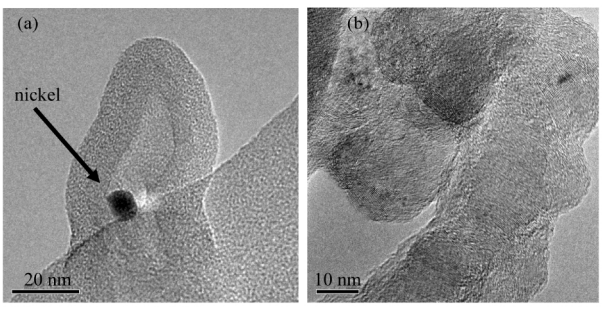

Fig.2 Typical TEM images of the microstructure of multi-walled carbon nanotubes (a) before and (b) after 20 min of CrO_3+HNO_3 solution treatment

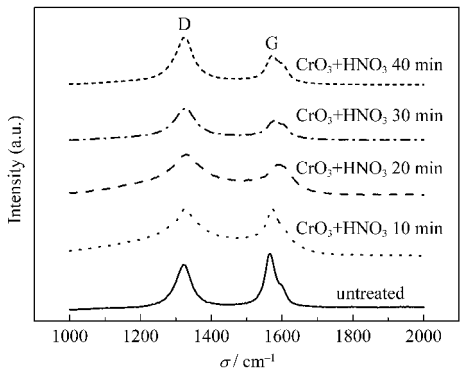

Fig.3 Raman spectra of the CNTs with different CrO_3+HNO_3 solution treatment times

Table 1 Positions of D and G peaks, and values of I_D/I_G ratios for CNTs untreated and treated with CrO_3+HNO_3 solution for various periods of time

t/min	σ_D/cm^{-1}	σ_G/cm^{-1}	I_D/I_G
0	1320	1564	0.839
10	1327	1571	1.003
20	1330	1585	1.250
30	1327	1573	1.481
40	1333	1584	1.670

of the amount of disorder in the nanotube materials. The I_D/I_G ratios are further summarized in Table 1, and are 0.839, 1.003, 1.250, 1.481, and 1.670 for the samples treated for 0, 10, 20, 30, and 40 min, respectively. The I_D/I_G ratio increased with the increase of CrO_3+HNO_3 duration indicating the increase of the defects and nano-nodes more specifically. Previous studies have shown that the D peak is associated with defects in graphite crystals in the material[19], while the G peak is related to graphite or graphite-structured carbon[22]. Hence, it can be found from the Raman spectra that after CrO_3+HNO_3 treatment, not only the tips are open-ended, but also some defects in graphite crystals are exposed on the top layer, which in turn makes the intensity of I_D increase, I_G decrease, and causes the ratio I_D/I_G to increase. For CNTs treated in CrO_3+HNO_3 solution, there is an increase in the ratio I_D/I_G indicating that their crystallinity degrades.

This can be attributed to the defect and amorphous carbon layer formed on the surface of CNTs. In addition, for CNTs treated in CrO_3+HNO_3 solution, there is an increase in the ratio I_D/I_G indicating that the purity of CNTs decreases. Based on the above observations, it can be concluded that amorphous carbon and CNTs were digested and attacked by CrO_3+HNO_3 treatment, and some CNTs were converted into defects and amorphous carbon nano-particles. This result is consistent with the SEM and TEM studies, as illuminated in Figs.1 and 2.

Table 2 shows the mass percentages of C, Si, and Ni as measured from EDS for the CNTs treated with CrO_3+HNO_3 for various periods of time. In Table 2, the same results measured for the CNTs treated with CrO_3 (0.4 mol·L^{-1}) are also included as a comparison. It can be seen in Table 2 that the mass percentage of Ni catalyst particles decreased to 0% after nitric acid solution treatment. This is a clear indication that the catalyst metal Ni on top of the tips of CNTs was dissolved and removed immediately in HNO_3 acid. The removal of exposed Ni is accomplished in the first step. It is also found in Table 2 that the mass percentage of carbon for the CNTs treated with CrO_3+HNO_3 acid is substantially higher than that of untreated CNTs. There is an abrupt increase in the mass percentage of carbon from 68.79% for as-grown CNTs to 79.27% for CNTs after 10 min of CrO_3+HNO_3 treatment. After 30 min of CrO_3+HNO_3 treatment, the removal of amorphous carbon nano-particles and CNTs becomes obvious and the mass percentage of carbon gradually decreases afterwards. Presumably, the slight decrease in the mass percentage of carbon reflects the fact that CNTs are under attack by CrO_3 acid and carbon atoms are removed in this process.

Table 2 Mass percentages (%) of C, Si, and Ni measured from EDS for CNTs treated with CrO_3+HNO_3 solution for various times

t/min	CrO_3 treatment			HNO_3+CrO_3 treatment		
	C	Si	Ni	C	Si	Ni
0	68.79	21.40	9.81	68.79	21.40	9.81
10	78.49	15.33	6.45	79.27	20.73	0
20	77.92	16.64	6.44	88.80	11.20	0
30	76.03	15.57	7.40	79.57	20.43	0
40	75.24	18.39	6.47	76.33	23.67	0

From the analyses of SEM, TEM, Raman spectroscopy, and EDS, it is found that amorphous carbon nano-particles and CNTs can all be dissolved and modified by CrO_3+HNO_3 treatment. However, their reaction rates with CrO_3+HNO_3 acid are quite different. Therefore, depending on the treatment time used, CrO_3+HNO_3 treatment can be divided into three stages: in the first stage, exposed catalyst metal is removed by HNO_3 immediately; in the second stage, amorphous carbon is dissolved and modified and CNTs are digested and conglomerated; and in the third stage, CNTs and amorphous carbon nano-particles are further digested and are eventually removed completely. Hence, with appropriate CrO_3+HNO_3 treatment time, the surface morphology of CNTs can be immensely modified. It is therefore expected that their field emission characteristics should also be varied to some extent.

The field emission characteristics of CNTs can be affected by various factors including their surface morphologies as well as the structural properties. Fig.4 shows the current density *versus* applied electric field (J–E) curves of the CNT films before and after CrO_3+HNO_3 treatment. From Fig.4, it is clearly seen that CNTs treated for 20 min have the highest emitted currents and the lowest turn-on electric field, whereas CNTs treated for 40 min have the lowest emitted currents and the highest turn-on electric field. For CNTs treated for 20 min in CrO_3+HNO_3 solution, the emitted currents were enhanced by more than one order of magnitude compared with those of untreated CNTs. Several factors contribute to this large increase in emitted currents for CNTs treated for 20 min. The increase in the surface density of CNTs owing to conglomeration phenomenon can provide plenty

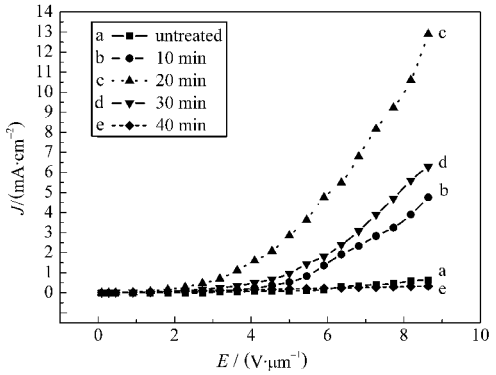

Fig.4 Current density *versus* applied electric field (J–E) characteristics of CNT films with different CrO_3+HNO_3 solution treatment times

of potential emission sites. The removal of catalyst metal results in the open-tipped CNTs, which are favorable for field emission, and the removal of surface states caused by nickel and amorphous carbon originally covering the surface of CNTs also assist the emission. On the other hand, the decrease in the emitted current for CNTs treated for 40 min is primarily caused by the removal of CNTs after prolonged reaction with CrO_3+HNO_3.

The CNTs were also treated with CrO_3 or HNO_3 alone to unambiguously determine their individual effects on the field emission of CNTs. Fig.5 shows the current density *versus* applied electric field (*J*–*E*) curves for four different CNT films: untreated, treated with HNO_3, CrO_3, or CrO_3+HNO_3 under the same conditions (at room temperature for 20 min). Compared with those of untreated CNTs, there is only a slight increase in the emitted currents for CNTs treated with HNO_3. However, more than one order of magnitude of increase is observed for CNTs treated with CrO_3 solution. CNTs treated with CrO_3+HNO_3 are found to exhibit the largest increase in the emitted currents. The material properties of CNTs can also be modified by acidic treatment. Fig.6 shows the Fowler-Nordheim (F-N) plot in which the field emission characteristics in the high field region are plotted as $\ln(J/E^2)$ *vs* $1/E$. The near straight-line relation in the high electric field region is a strong indication that the emitted currents are dominated by field emission, and the slopes can be used to determine the geometric field enhancement factors (β) of CNTs[23]. The exact values of β can be derived as $0.95B\varphi^{3/2}d/b$, where, B=6.87×10^7 (C^2·cm$^{1/2}$)$^{-1}$, b is the slope in the high electric field region, and d is the distance between cathode and anode, which is 110 μm in this study. Assuming a work function (φ) of ca 5 eV, the β values can be derived from the slopes of the F-N plots. The β values obtained for the as-grown and treated with HNO_3, CrO_3, and CrO_3+HNO_3 samples were 9001, 12290, 19075, and 25491 cm^{-1}, respectively.

It seems that the primary function of HNO_3 is to attack catalyst metal. The removal of catalyst metal results in the open-tipped CNTs, which are favorable for field emission. Several factors contribute to this large increase in emitted currents for CNTs treated in CrO_3+HNO_3 solution. After acidic treatments, the surface morphology of CNTs is totally varied and the surface

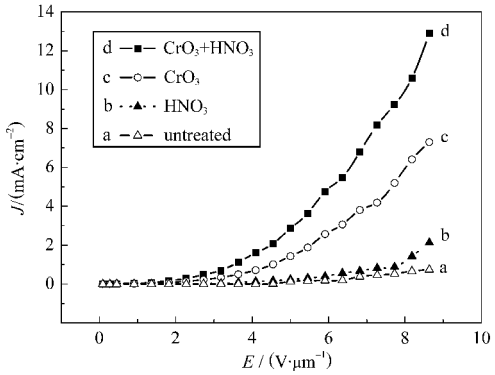

Fig.5 Current density *versus* applied electric field (*J*–*E*) curves for CNT films treated with different acid solutions at room temperature for 20 min

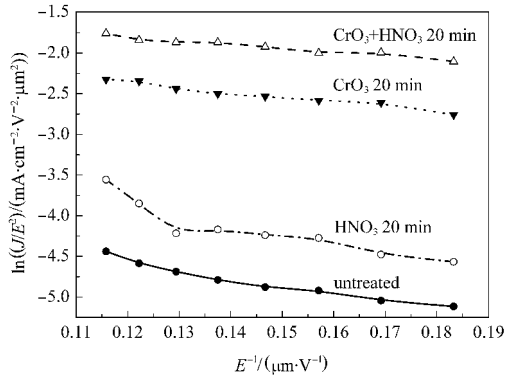

Fig.6 Corresponding Fowler-Nordheim plots at high electric fields for the *J*–*E* characteristics shown in Fig.5

density of emission sites is increased by conglomeration phenomenon. In addition, the local field enhancement induced by the highly curved CNT surface can also assist the emission. These factors altogether cause the enhancement in field emission for the CNTs treated with CrO_3+HNO_3.

3 Conclusions

In this study, we have demonstrated a novel technique using CrO_3+HNO_3 mixed solution to modify synthesized CNTs. This simple technique allows the functionalization of multi-walled carbon nanotubes in a fast and controllable manner. Compared with CNTs treated with HNO_3, the CNTs treated with CrO_3+HNO_3 mixed solution exhibit a higher emission current and a lower turn-on electric field. SEM, TEM, EDS, and Raman spectroscopic studies have shown that amorphous carbon and CNTs can all be modified and removed by CrO_3+HNO_3 treatment. However, owing to their different reaction rates, the surface morphology, structural properties, and chemical compositions of CNTs will vary with CrO_3+HNO_3 treatment time. Therefore, with appropriate treatment time, e.g. 20 min in this study, the emitted currents can be enhanced by more than one order of magnitude. This large increase in emitted current after 20 min of CrO_3+HNO_3 treatment can be attributed to the increase of CNT surface density and favorable surface morphology, which results in the increase in the field enhancement factors of CNTs. On the other hand, prolonged CrO_3+HNO_3 treatment (e.g. 40 min) removes CNTs eventually, and thus results in a decrease in field emission.

References

1 Iijima, S. *Nature*, **1991, 354**: 56
2 de Heer, W. A.; Chatelain, A.; Ugarte, D. *Science*, **1995, 270**: 1179
3 Dean, K.; Chalamala, B. *Appl. Phys. Lett.*, **1999, 75**: 3017
4 Bonard, J. M.; Kind, H.; Stockli, T.; Nilsson, L. O. *Solid-State Electron.*, **2001, 45**: 893
5 Hamwi, A.; Alvergnat, H.; Bonnamy, S.; Beguin, F. *Carbon*, **1997, 35**: 723
6 Petit, P.; Mathis, C.; Journet, C.; Bernier, P. *Chem. Phys. Lett.*,

1999, 305: 370

7 Kazaoui, S.; Minami, N.; Jacquemin, R.; Kataura, H.; Achiba, Y. *Phys. Rev. B*, **1999, 60**: 13339

8 Cao, L. C.; Liu, Y. Q.; Wang, Y.; Wei, D. C.; Fu, L.; Hu, P. A.; Zhang, H. L.; Huang, L. P.; Yu, G. *Acta Phys. -Chim. Sin.*, **2008, 24**(6): 951 [曹灵超, 刘云圻, 王 钰, 魏大程, 付 磊, 胡平安, 张洪亮, 黄丽平, 于 贵. 物理化学学报, **2008, 24**(6): 951]

9 Mittal, J.; Monthioux, M.; Allouche, H.; Stepan, O. *Chem. Phys. Lett.*, **2001, 339**: 311

10 Qiu, K. D.; Li, W. B. *Acta Phys. -Chim. Sin.*, **2006, 22**(12): 1542 [裘凯栋, 黎维彬. 物理化学学报, **2006, 22**(12): 1542]

11 Dresselhaus, M. S.; Dresselhaus, G. *Adv. Phys.*, **2002, 51**: 1

12 Lee, Y. H.; Jang, Y. T.; Kim, D. H.; Ahn, J. H.; Ju, B. K. *Advanced Materials*, **2001, 13**: 479

13 Chambare, P. D.; Qian, D.; Dickey, E. C.; Grimes, C. A. *Carbon*, **2002, 40**: 1903

14 Chang, X. M. Master Dissertation. Taiwan: Dayeh University, 2006 [张轩铭. 硕士学位论文. 台湾: 大叶大学, 2006]

15 Yang, Z. H.; Li, X. H.; Wang, H. Q. *Chemistry World*, **1999, 12**: 627

16 Li, X. H.; Yang, Z. H.; Chen, Z. G.; Wang, H. Q.; Li, T. B.; Sheng, N. Y.; Li, J. *Chinese New Carbon Materials*, **1999, 14**(3): 32 [李新海, 杨占红, 陈志国, 王红强, 李添宝, 沈宁一, 李 晶. 新型炭材料, **1999, 14**(3): 32]

17 Kung, S. C.; Hwang, K. C. *Appl. Phys. Lett.*, **2002, 80**: 4819

18 Zhi, C. Y.; Bai, X. D.; Wang, E. G. *Appl. Phys. Lett.*, **2002, 81**: 1690

19 Ahn, K. S.; Kim, J. S.; Kim, C. O.; Hong, J. P. *Carbon*, **2003, 41**: 2481

20 Kawabata, A.; Ota, K.; Matsuura, T.; Urayama, M.; Murakami, H.; Kita, E. *J. Appl. Phys.*, **2002, 41**: 1363

21 Chakrapani, N.; Curran, S.; Wei, B.; Ajayan, P. M. *J. Mater. Res.*, **2003, 18**: 2515

22 Nilsson, L.; Groening, O.; Emmenegger, C.; Kuettel, O.; Schaller, E.; Schlapbach, L.; Kind, H.; Bonard, J. M.; Kern, K. *Appl. Phys. Lett.*, **2000, 76**: 2071

23 Gadzuk, J. W.; Plummer, E. W. *Rev. Mod. Phys.*, **1973, 45**: 487